Carbohydrate Polymers 118 (2015) 107–114

Contents lists available at ScienceDirect

Carbohydrate Polymers

journal homepage: www.elsevier.com/locate/carbpol

Water-induced local ordering of chitosan polymer chains in thin layer films

Claire Madeleine-Perdrillat[a], Thomas Karbowiak[a,*], Jesus Raya[b], Régis Gougeon[a], Philippe R. Bodart[c], Frédéric Debeaufort[a]

[a] UMR A 02.102 PAM, Université de Bourgogne/AgroSup Dijon, Equipe PAPC, 1 esplanade Erasme, F-21078 Dijon, France
[b] Univ Strasbourg, Inst Chim, UMR CNRS 7177, BP 296, F-67008 Strasbourg, France
[c] IUT A – Université des sciences et technologies de Lille, F-59653 Villeneuve d'Ascq, France

ARTICLE INFO

Article history:
Received 28 August 2014
Received in revised form 31 October 2014
Accepted 3 November 2014
Available online 7 November 2014

Keywords:
Water
Structure
Polymer
Chitosan
NMR

ABSTRACT

Carbon-13 NMR (CP-MAS and FSLG ^{1}H–^{13}C HETCOR) have been applied to chitosan salt films synthesized in acetic acid and exposed to different relative humidity environments (32% or 75%) at 20 °C for 1 month. It gives insight in the relationship between structure and functional properties according to the hydration level of this biomaterial as a film. The acetate ions trapped in the chitosan act as structuring agents between chitosan chains for the low hydration state. But, increasing the moisture content induces spontaneous removal of acetic acid and a subsequent modification in the film structure, with an increase in local ordering. HETCOR experiments also showed a multiplicity of signals for most of the observed carbon atoms and in particular those implied in the glycosidic linkage, which reveals different water-induced conformational states. Changing the water content allows to modify the polymer structure and therefore to modulate the properties such as controlled release of active compounds trapped in chitosan-based coatings, e.g., for medicated dressing or active packaging.

1. Introduction

Chitin is the second most abundant polysaccharide in nature after cellulose. Its estimated worldwide production is 10^{10}–10^{12} tons per year (Kumar, 2000). It generally comes from crustacean shells, insects, or mollusks. Chitin is a linear polymer of β-(1–4)-N-acetyl-D-glucosamine units. Chitosan is obtained from chitin by deacetylation in the presence of base agents, which gives a copolymer of glucosamine and N-acetylglucosamine units. This polymer contains three different polar functional groups, namely, hydroxyl (OH), primary amine (NH_2), and ether (C—O—C) groups, plus depending on the deacetylation level residual carbonyl (C=O) groups. The presence of these functional groups gives chitosan high water attracting capacity. Due to its positive charge on the amino group under acidic conditions, chitosan is often referred to as cationic polymer, which can easily bind to negatively charged molecules. This property, along with its biocompatibility, makes chitosan a very attractive polymer in various fields, such as in food and nutrition (edible film (Dutta, Tripathi, Mehrotra, & Dutta, 2009; Shahidi, Arachchi, & Jeon, 1999), antimicrobial film (Dutta et al., 2009)), in biotechnology (artificial skin, reconstituted tissue structure (Di Martino, Sittinger, & Risbud, 2005)), in material science, for drugs and pharmaceuticals (encapsulating material (Rinaudo, 2006)), in agriculture and environmental protection (chitosan membranes (Peter, 1995)), and recently in gene therapy (Kumar, 2000; Rinaudo, 2006).

The structure of chitosan has been investigated in aqueous solutions and solid state by various spectroscopic techniques (NMR (Domján, Bajdik, & Pintye-Hodi, 2009; Heux, Brugnerotto, Desbrieres, Versali, & Rinaudo, 2000; Webster, Osifo, Neomagus, & Grant, 2006), IR (Brugnerotto et al., 2001; Cárdenas, Cabrera, Taboada, & Miranda, 2004; Harish Prashanth, Kittur, & Tharanathan, 2002; Rinaudo, 2006), X-ray spectroscopy (Clark & Smith, 1937; Ogawa, Yui, & Okuyama, 2004; Okuyama, Noguchi, Miyazawa, Yui, & Ogawa, 1997; Saito, Tabeta, & Ogawa, 1987)) and by molecular modeling (MD simulation (Franca, Lins, Freitas, & Straatsma, 2008; Prathab & Aminabhavi, 2007), MM2 (Ferreira, Pedroni, Alimenti, Gschaider, & Schulz, 2008)). Main results obtained on crystals showed that fully deacetylated chitosan develops many types of structural complexes through several systems of intra and intermolecular hydrogen bonds. This polymorphism (Rinaudo, 2006)

Abbreviations: CS, chitosan (powder); CSF3, chitosan film equilibrated at 32% relative humidity (during 1 month); CSF7, chitosan film equilibrated at 75% relative humidity (during 1 month).

* Corresponding author. Tel.: +33 3 80 77 23 88; fax: +33 3 80 77 40 47.
E-mail address: thomas.karbowiak@u-bourgogne.fr (T. Karbowiak).

http://dx.doi.org/10.1016/j.carbpol.2014.11.001
0144-8617/

can be classified into three types (Ogawa et al., 2004): (i) an anhydrous form in which the polymer backbone chains is an extended 2-fold helix (type I) (Yui et al., 1994); (ii) a hydrated crystal form with a different (relaxed-) 2-fold helix (type II) (Kumirska et al., 2010; Lertworasirikul, Tsue, Noguchi, Okuyama, & Ogawa, 2003; Okuyama et al., 2000); (iii) a chain pattern with an extended 5-fold helix with an asymmetric unit of one glucosamine (type III) (Cunha et al., 2012). Few structural data are available for an intermediate state, which can be referred to as low hydrated state. This last case covers a large range of applications of chitosan polymer in its uses as films, coatings, or encapsulation agent for controlled release of drug.

The good mechanical properties of chitosan films, comparable to many medium-strength commercial synthetic polymers, as well as the excellent oxygen-barrier properties in dry conditions, are closely related to its structure, and in particular to the hydrogen bonds network (Epure, Griffon, Pollet, & Avérous, 2011). The relationship between such properties and the polymer structure under various environmental conditions (water content, charge of the polymer, presence of other small solutes, pH) requires a better knowledge. The hydroxyl groups (a primary hydroxyl in C6 and a secondary hydroxyl in C3) and the highly reactive amino group in C2 concomitantly participate in intra- and intermolecular hydrogen bonds, resulting in the formation of different polymorphic forms whose properties may vary considerably.

The influence of water/acetate ion on the structure of chitosan is investigated in the present work on a molecular scale with solid state NMR. It aims at comparing a weakly hydrated state of chitosan film to a more hydrated state, focusing in particular on the hydrogen bond network. It is particularly interesting in order to get better insight in the relationship between structure and functional properties to target controlled release applications of active compounds from the chitosan layer (film or coating), for the pharmaceutical or the food industries. ^{1}H–^{13}C Cross Polarization Magic Angle Spinning (CP-MAS) is very sensitive to changes in the H-bonded structure of chitosan (Heux et al., 2000; Kameda, Miyazawa, Ono, & Yoshida, 2005) and two-dimensional (2D) spectroscopy gives further insights in the interactions between molecules. In particular, Frequency-Switched Lee–Goldberg (FSLG) ^{1}H–^{13}C Heteronuclear Correlations (HETCOR) NMR has been previously used to study the effect of plasticizers on chitosan film with 50% acetylation degree, dried 24 h at 50% Relative Humidity (RH), at a MAS frequency of 10 kHz, unraveling different mechanisms of plasticization though induced mobility and specific interaction with the polymer according to the type of plasticizer used (glycerol or polyethylene glycol) (Domján et al., 2009). The same technique, at a higher MAS frequency (18 kHz) is used in this study in order to better understand the influence of water/acetate ion on hydrogen bonding structure of chitosan-based film having an acetylation degree of 10%.

2. Materials and methods

2.1. Materials

Chitosan (CS) used for this study is a commercial grade supplied by France Chitine, powder 652, having a molar mass of 165 kg mol^{-1}. Its degree of deacetylation is approximately 90% (data given by the supplier). Table 1 gives the major ions present in the initial chitosan powder. A 2% (v/v) acetic acid (glacial 100%, Merck, Darmstadt, Germany) solution (pH 4.5) was used as dissolution medium for chitosan. Films were obtained by casting method followed by solvent evaporation in a ventilated climatic chamber (KBF 240 Binder, ODIL, France) under controlled conditions of temperature (20 °C) and relative humidity (30%). Their thickness is around 60 μm.

Table 1
Anions and cations in the initial chitosan powder (CS).

Ion	Concentration (mg/g)	Method
Chloride	21.42	Ionic chromatography
Sulfate	0.53	
Sodium	102.80	Inductively coupled plasma atomic emission spectroscopy
Potassium	5.23×10^{-3}	
Copper	1.22×10^{-3}	
Iron	1.50	
Platinum	$<0.5 \times 10^{-3}$	High-resolution continuum source atomic absorption spectroscopy

2.2. Film equilibration

For studying the effect of relative humidity on chitosan-based films, the films were exposed to ambiances with temperature and relative humidity controlled conditions for 1 month to ensure equilibration. To that purpose films were stored in air-tight cabinet containing saturated salt solutions of NaCl or $MgCl_2$ (Sigma–Aldrich) to fix the relative humidity at 75 ± 0.5% and 32 ± 0.5%, respectively. Cabinets were stored in a chamber (KBF 240 Binder, ODIL, France) which temperature is regulated at 20 ± 0.5 °C. These films stored at 75% or 32% RH were designed hereafter as CSF7 and CSF3, respectively.

As determined by Karl Fischer titrimetry, the water content (wt%, dry basis) was 6.45 (±0.12) for the chitosan powder, 19.66 (±1.09) and 5.28 (±0.82) for CSF7 and CSF3 films, respectively.

Films were chopped before being inserted into NMR rotors.

2.3. Elemental analysis

Elemental analysis was done using a Flash EA 1112 CHNS/O analyzer from Thermo Electron Corporation. It aims at determining the acetate ion acid content in chitosan film from the *C*/*N* ratio.

2.4. Solid state NMR spectroscopy

^{1}H–^{13}C CP-MAS spectra were recorded on a Bruker 300 spectrometer operating at frequencies of 300.1 and 75.5 MHz for ^{1}H and ^{13}C, respectively, at a temperature of 20 °C. The spectra were acquired with a 4-mm MAS probe at a spinning speed of 10 kHz. Hartmann–Hahn matching for the ^{1}H–^{13}C CP-MAS experiments was set on adamantane for ^{1}H and ^{13}C radio-frequency fields of ca. 60 kHz. Chemical shifts for ^{1}H and ^{13}C spectra were referenced to the signal of water (4.87 ppm) and to the methylene signal of adamantane (29.47 ppm), respectively. 360 transients were collected with a contact time of 1 ms and a recycling delay of 2 s, except for the sample CSF3 (5 s). No line broadening was applied during the processing.

Two dimensional FSLG ^{1}H–^{13}C HETCOR spectra were recorded on a Bruker 500 spectrometer with a 3.2-mm MAS probe at spinning speed of 18 kHz, at a temperature of 20 °C. 360 transients were collected with a contact time of 1 ms and a recycling delay of 2 s for each of the 128 increments recorded with an indirect window size of 16 kHz. SPINAL-64 proton decoupling with a strength of 70 kHz was used during the acquisition. Contour plots are constituted of 20 levels on a logarithm scale from 0.07 to 1. A 20 Hz Lorentzian line broadening in the direct dimension was applied during the processing. All spectra have been normalized independently to unity.

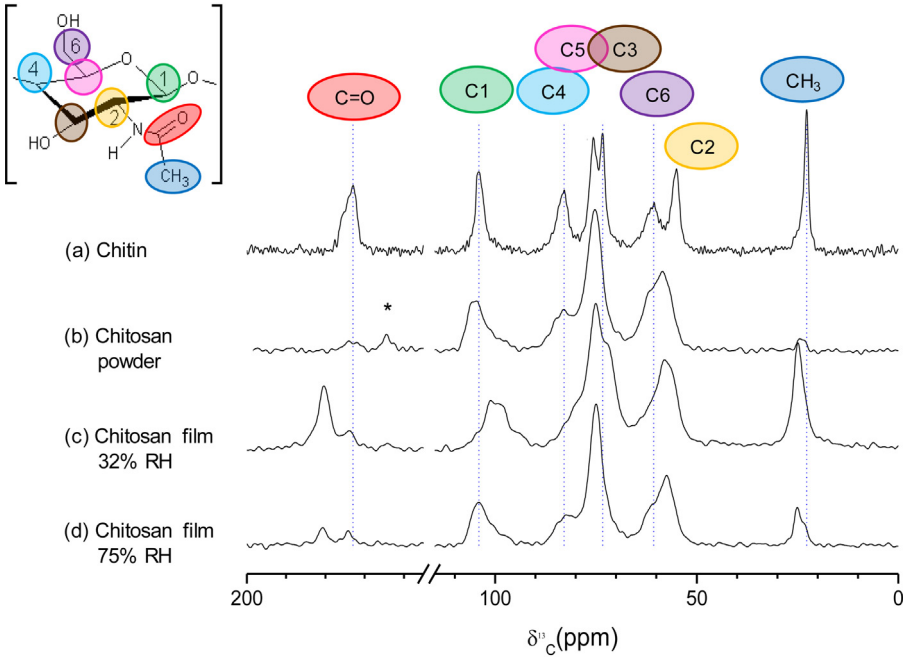

Fig. 1. ^{13}C CP MAS spectra of chitin (a), chitosan powder (b), film equilibrated at 32% (c) and 75% RH (d), at 20 °C.

3. Results and discussion

Chitin has been chosen as a reference standard compound in order to fully identify the structural modifications occurring in chitosan after deacetylation. Chitin has three known crystalline allomorphs (α-, β- and γ-chitin). α-Chitin is the most thermodynamically stable and the most abundant (Kameda et al., 2005). The ^{1}H–^{13}C CP-MAS NMR spectra of α-chitin (hereafter named chitin), of chitosan in the form of powder (CS) and of films equilibrated either at a relative humidity of 32% (CSF3) or 75% (CSF7) are displayed in Fig. 1 with the conventional assignments (Tanner, Chanzy, Vincendon, Roux, & Gaill, 1990). Chemical shifts are reported in Table 2.

The ^{13}C NMR spectrum of chitin shows eight well-defined resonance peaks corresponding to C1–C6 carbons of the chitosan monomer and acetyl groups (Kameda et al., 2005; Tanner et al., 1990; Zhang, Haga, Sekiguchi, & Hirano, 2000). Peaks at 22.7 and 173 ppm are ascribed to methyl and carbonyl carbons, respectively. This last one is very sensitive to the hydrogen bond structure. It can be deconvoluated into two peaks corresponding to two different types of hydrogen bonds involving N-acetyl groups: intramolecular with the C6 hydroxymethyl groups (C6OH···O=C) and intermolecular with amine groups NH···O=C (Kameda & Ando, 1997; Kameda et al., 1996; Kameda, McGeorge, Orendt, & Grant, 2004; Kameda et al., 2005). N-acetyl groups located along the chitin polymer are known to ensure a strong cohesion and stability of the macromolecular edifice (Ogawa et al., 2004). The carbons in the repeating units of chitin are detected between 55 and 105 ppm. The carbon C2, bonded to the N-acetyl group, gives a chemical shift at 55 ppm. The C6, corresponding to the pendant hydroxymethyl group, resonates at 60.6 ppm. The broader signal observed for C6 may be attributed to two distinct conformations for the C6—O6 hydroxyl group (Kono, 2004; Sikorski, Hori, & Wada, 2009). The rather close chemical shifts at 73.4 and 75.6 ppm are assigned to C3 and C5 pyranose carbons, respectively. A hydroxymethyl is bonded to C5, while a hydroxyl is attached to C3. The carbons involved in the glycosidic linkage, namely C4 and C1, exhibit chemical shifts at 82.9 and 104.5 ppm, respectively.

Chitosan spectra are less resolved than the chitin one (Fig. 1). This indicates a lower ordering structure, which obviously comes from the modification of the hydrogen bond network existing through N-acetyl groups (Franca, Freitas, & Lins, 2011). However, the same line width for CS and the films indicate that on the length scale probed by NMR, the local order is comparable. In the CS spectrum, signals of the acetyl carbons (24.5 and 174.1 ppm) have strongly decreased but have not vanished, indicating incomplete deacetylation of the chitin. The additional signal at 165.1 ppm (labeled with an asterisk) is attributed to some residual carbonyl groups from impurities. Nevertheless, all chemical shifts are in line with those obtained for purified chitosan (Heux et al., 2000), as reported in Table 2. The most abundant hydrated polymorph of chitosan (corresponding to the CS sample) has an extended two-fold

Table 2
Comparison in ^{13}C CP-MAS chemical shifts of highly purified chitosan obtained by Heux et al. (2000) and from this study using values from deconvolution of the spectra for chitin, and line position for chitosan powder and chitosan films (CS, chitosan powder; CSF3, film equilibrated at 32% RH; CSF7, film equilibrated at 75% RH).

	C=O		C1	C4	C5	C3	C6	C2	CH_3
Chitin	173.0		104.5	82.9	75.6	73.4	60.6	55.0	22.7
CS	174.1		104.7	83.0	75.3[a]		61.7[b]	58.5	24.5
CS (from Heux et al.)	*173.6*		*104.7*	*82.4*	*75.0*		*60.1*	*57.6*	*23.2*
CSF3	180.4	174.0	101.1	–	75.1	72.4[b]	–	58.0	24.9
CSF7	180.7	174.3	104.1	82.4	75.0[a]		61.6[b]	57.5	25.1

Line position (ppm):
[a] C3 and C5 signal are overlapping,
[b] position of a shoulder.
When no maximum or shoulder was unambiguously identified, no chemical shift is reported.

helix (type II). Chitosan chains are packed along the *c*-axis in an antiparallel fashion, and these chains are hydrogen bonded along the *b*-axis to make a sheet structure, which is stacked along the *a*-axis. The crystal structure is stabilized by water molecules located between the sheets. It is possible to produce an anhydrous polymorph by an irreversible annealing process. The resulting structure is also formed of antiparallel chains but there is no water molecule in the structure. In that case, chains having parallel directions are bonded by direct H-bond to make a sheet and neighbor sheets having antiparallel directions are stacked (Ogawa et al., 2004).

CSF3 and CSF7 samples are chitosan acetic acid salts, since fully fresh deacetylated chitosan acetic salt has a structure of sheets of glucosamine polymer (type II), CSF3 and CSF7 with an acetylation degree of 10% are expected to have a structure close to this hydrated type II form, for which a plausible structure is a relaxed-two-fold helix with an asymmetric unit of four glucosamine units in which water and $C_2H_3O_2^-$ anions are present and stabilize the structure (Okuyama et al., 2000). However, it is worth noting that anhydrous chitosan crystals can be obtained at room temperature by spontaneous removal of the acid accompanied by dehydration of several monocarboxylic acids. In the particular case of chitosan acetic salts, the salt freshly prepared gave a fiber pattern of type II but when this sample was stored at room atmosphere for 6 months (Demarger-Andre & Domard, 1994) or at 100% RH for 1 month (Ogawa et al., 2004) the resulting product was similar to the anhydrous polymorph of annealed chitosan. The higher the RH the faster the conversion occurs. With our samples stored 1 month at 32% and 75% RH we are probing on films the structural change from chitosan type II to annealed chitosan.

The chemical shifts obtained in the spectra for chitosan (CS) and chitosan films (CSF3 and CSF7) displayed in Fig. 1 are in accordance with those recorded by Domján et al. (2009) for 50% deacetylated chitosan and films synthesized with ascorbic acid and dried at 50% RH for 24 h, except for the C6–C2 peaks which are slightly less resolved here. For CSF3 and CSF7 spectra, two lines are observed for the carbonyl atoms. The weaker signal at 174 ppm is attributed to residual N-acetyl groups as previously observed in CS, while the line at 180.5 ppm is attributed to acetate groups trapped in the films. This is supported by the asymmetric shape of the methyl carbon signal at 25 ppm: the shoulder visible in CSF7 is attributed to N-acetyl groups while the higher peak is attributed to acetates.

In Fig. 1, carbonyls from N-acetyl groups are clearly distinct from carbonyls of acetate ions. According to Heux et al. (2000), the degree of acetylation, as well as the amount of acetate ions in the films, can therefore be evaluated. After deconvolution of the spectra, it is expressed as the ratio of the surface areas of each of these two C=O signals over the surface area of the polysaccharide backbone signal. Calculated values are reported in the first column of Table 3. In the CS sample, the measured degree of acetylation is close to the value given by the supplier (10%). Doing the same calculation from the chitin spectrum gives a value of 106% instead of the expected 100%. However, for chitosan films CSF3 and CSF7, this percentage of N-acetyl groups is found to be 20% and 17%, respectively. This is inconsistent with the acetylation degree of the initial chitosan powder (10%). It seems reasonable to ascribe such discrepancy to the non-quantitative nature of the cross polarization experiment rather than to the formation of acetamide during the film synthesis, although this might not be fully excluded since a similar reaction (formation of formamide) has been proposed in the case of chitosan synthesized in formic acid (Demarger-Andre & Domard, 1994). On four chitosan samples with different acetylation degrees (0, 20, 60, 100%), Heux et al. (2000) have shown that solid state ^1H–^{13}C CP-MAS NMR can provide accurate determination of the acetylation degree, in accordance with ^1H liquid sate NMR measurement. However, if the samples differ (i.e., films/chitosan powder), in particular if carbonyls are not in the same proton environment in terms of dynamics, proton population and carbon–proton distances, the CP MAS spectra may not be quantitative from one sample to another. Indeed, in CSF3 and CSF7 the acetylation degree measured by CP-MAS (20% and 17%, respectively) are of the same order because both samples are issued from the same production method (only the final exposure to water vapor varies) and similar carbonyl proton surrounding may occur in the samples. However, films differ sufficiently enough from the starting chitosan powder to give CP-MAS spectra which cannot be quantitatively compared to the chitosan or chitin CP-MAS spectra.

Intensities of carbonyl and methyl lines of the trapped acetates suggest that there is much more acetate in CSF3 than in CSF7. Quantitatively, the amount of trapped acetates is reduced by a factor 3.5 when going from CSF3 to CSF7 (Table 3). This is in good agreement with the decrease in acetate content by a factor 3.6 as measured by elemental analysis (Table 3). Even if water and acetic acid have close saturated vapor pressures at room temperature, in the studied system only the water vapor pressure is maintained constant but this is not the case for acetic acid. It suggests that during the storage of the films under this moisture-controlled atmosphere a removal of acetates is occurring when the film is stored at a high relative humidity, leaving the film in their volatile form as acetic acid. However it is difficult to ascertain if the exchanged proton comes from the amine group or from water, the corresponding NMR signals ($-NH_2$ and HO^-, respectively) being not (or barely in Fig. 3) visible. This spontaneous removal is increased when the amount of water is more important, as previously observed during the drying of fully deacetylated chitosan salt (Ogawa et al., 2004).

In Fig. 1, lines composing chitosan spectra (CS and CF) are asymmetric suggesting that several distinct surroundings exist for carbon atoms. Water has a major effect on C1, C3, C4 and C6 carbon atoms. A +3 ppm shift is observed for C1 signals when relative humidity for film storage increases from 32% to 75%. Comparable shifts can also be estimated for C3, C4 and C6 signals. In CSF3, the C3 signal observed as a shoulder (upfield shift of −2.7 ppm) of the C5 line, is completely shifted in the C5 band and disappears when the amount of water increases to 75% for CSF7. On the contrary, for C4 and C6 bands, which overlap with adjacent C5 and C2 signals in CSF3, the increase in water content moves the lines to higher chemical shifts and a more resolved spectrum is produced for CSF7. Saitô et al. (Saito et al., 1987) have shown that the ^{13}C chemical shifts of C1 and C4 carbon atoms in chitosan acid salts vary by up to 8 ppm according to the two torsion angles in the glycoside bond $C1—O_{gly}(\varphi)$ and $O_{gly}—C4(\psi)$. In the proposed Type II structure, at least two very different torsion angles are expected since two adjacent pyranose rings are either parallel or perpendicular. Moreover, these torsion angles depend on the influence on the hydrogen bond structure of molecules present between the chains (H_2O/acetate ions). Some investigations by infra-red spectroscopy, as in the case of hyaluronan polymer, might help in better characterizing these interactions (Haxaire, Maréchal, Milas, & Rinaudo, 2003). In Fig. 1, C1 and C4 signals are likely to result from the convolution of several lines dependent upon the water/acetate content. The chemical shift sensibility of C3 and C6 signals with the RH is also closely connected to the hydrogen bond structure. These two carbon atoms are directly bonded to a hydroxyl group which is involved in the H-bond structure. Consistently, since C5 and C2 atoms are not directly bonded to oxygen atom they are expected to be less affected and their signals appear at the same position in CSF3 and CSF7.

In order to increase the resolution and to assess to spatial connectivities, two-dimensional ^1H–^{13}C FSLG HETCOR experiments have been recorded. It is well known that for contact times lower than 0.1 ms, only strong correlations between ^1H and ^{13}C exist in directly bonded ^1H–^{13}C pairs (Kono, 2004; Van Rossum, Forster, & De Groot, 1997). When the contact time increases (0.5 ms and above) long range ^1H–^{13}C correlations and in particular

Table 3
Acetylation degree and relative amount of acetate ions, calculated from the ^{1}H–^{13}C CP-MAS NMR by the ratio of the surface areas of respective C=O signals over the polysaccharide backbone signal. Also indicated is the C/N ratio from elemental analysis in chitosan powder and films, which enables to calculating the number of moles of acetate ions per moles of chitosan monomer unit.

	CP-MAS NMR			Elemental analysis		
	Acetylation degree (%)	Acetate ions (%)	Acetate ions loss (%)	C/N ratio	Acetate ions/monomer unit (molar ratio)	Acetate ions loss (%)
CS	12			5.53		
CSF3	20	71		6.69	0.68	
CSF7	17	19	73.2	5.86	0.19	71.4

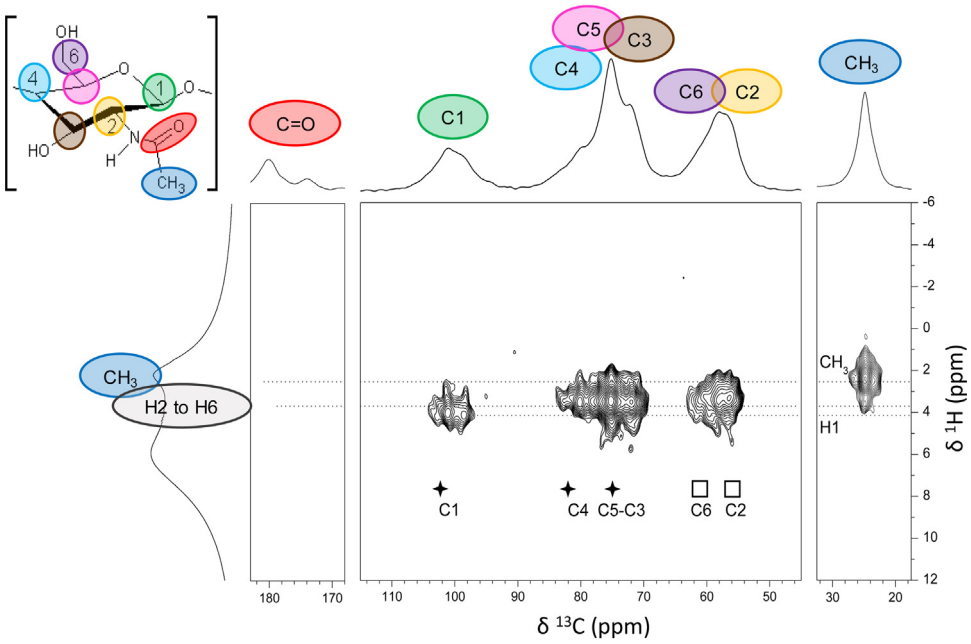

Fig. 2. 2D ^{1}H–^{13}C FSLG-HETCOR spectrum of chitosan film equilibrated at 32% RH and at 20 °C. One-dimensional spectra are ^{1}H direct polarization (4 transients collected with a 4 s recycling delay) and ^{13}C Cross polarization (contact time: 1 ms, recycling delay: 2 s, 6000 transients).

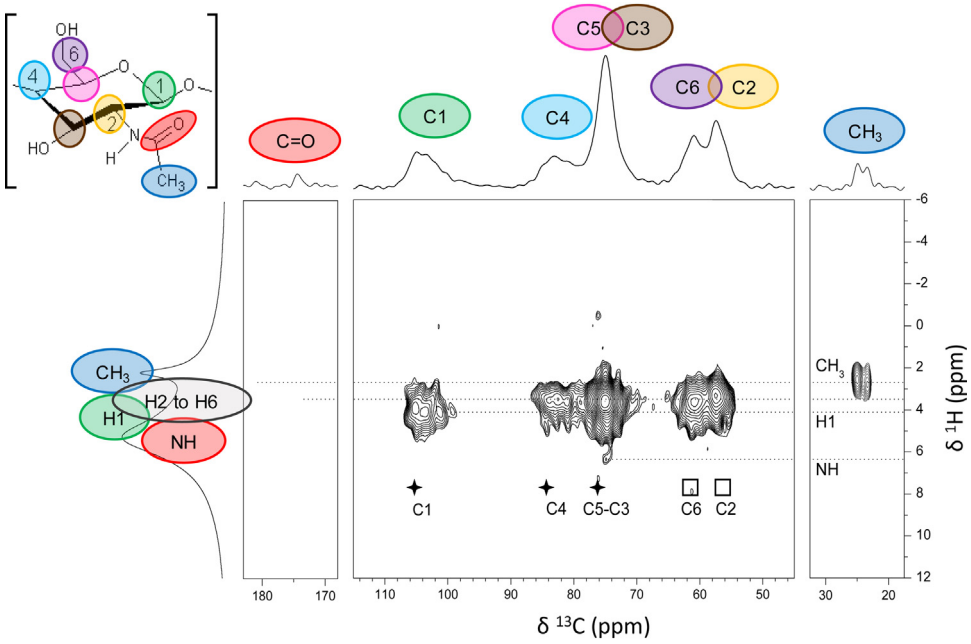

Fig. 3. 2D ^{1}H–^{13}C FSLG-HETCOR spectrum of chitosan film equilibrated at 75% RH and at 20 °C. One-dimensional spectra are ^{1}H direct polarization (4 transients collected with a 4 s recycling delay) and ^{13}C Cross polarization (contact time: 1 ms, recycling delay: 2 s, 2000 transients).

Table 4
Maximum peak positions (^{1}H chemical shift) in CSF3 and CSF7.

CSF3	^{13}C	OH	H1	H4	H5	H3	H6	H2	CH_3
C=O	180.1								3.7, 2.5
	174.0								
C1	103.4		4.0						
	101.1		4.0, 3.0						
	98.6		4.0						
C4	82.7			3.5					
	81.8			3.5					
	80.1			3.5					
C5	75.2	4.7			3.5				
C3	71.9	4.7				3.5			
C6	60.7						3.5		
C2	58.1	5.3						3.3	
	56.2							3.3	
CH_3	26.6								2.5
	24.8								3.4, 2.5, 0.3
	23.4								3.6

CSF7	^{13}C	NH	H1	H4	H5 & H3	H6	H2	CH_3
C=O	181.0							2.5
	174.0						3.4	
C1	105.3		4.1					
	104.0		4.1					
	101.5		4.2					
	99.5		4.2					
C4	84.2			3.5				
	82.6			3.5				
	80.9			3.5				
C5–C3	75.1	6.4			3.6			2.2
C6	60.7					3.6		
C2	57.4						3.4	3.3
	55.2						3.4	
CH_3	24.8							2.5
	23.3							2.7

intermolecular correlations are observable (Murata, Kono, Katoh, Kuroki, & Ando, 2003). HETCOR spectra of CSF3 and CSF7 (Figs. 2 and 3, respectively) were recorded with a contact time of 1 ms to favor the recording of long range interactions over interactions between protons directly bonded to carbon atoms. The spectra present similar features and are comparable with those recorded by Domján et al. (2009), however, the resolution achieved in our experiments unambiguously highlights the multiplicity of the sites that are responsible for the linewidth previously observed in Fig. 1. For both films, the HETCOR spectra reveal the existence of numerous correlations (Figs. 2 and 3 and Table 4).

In CSF3 (Fig. 2), no correlation for the carbonyl signal of N-acetyl groups is observed while two correlations are present for the carbonyl group (180.1 ppm) of acetate ions at 3.5 and 2.7 ppm. Moreover, the correlation signal of the methyl groups shows several peaks: a shoulder at 23.4 ppm is attributed to N-acetyl groups, the maximum signal at 24.8 ppm which consists of at least two cross-peaks at 3.4 and 2.5 ppm is attributed to acetate ions, as well as the weak peak at 26.6 ppm. The multiplicity of the correlations for the methyl group of the acetate ions present in CSF3 indicates that acetate ions are localized in at least two distinct defined surroundings. The stronger peaks at 2.5 ppm for methyl and carbonyl carbon atoms correspond to a correlation with protons of the methyl group, while the weaker peaks at 3.4 ppm could be attributed to correlations of the same carbon atoms with protons of the glucosamine unit. This confirms the inclusion of acetate ions between chitosan chains. Because of the weaker resolution of the proton dimension for the glycosidic unit carbon atoms, it is difficult to ascertain this correlation. Although there is a large amount of acetate ions in the system (Table 3), not all potential sites for electrostatic interactions with glycosamyl residues would be occupied (the molar ratio acetate ions/monomer unit is 0.68), even if considering the acetylation degree of 20% (Table 3). Despite such basic calculation, a population of acetate ions is electrostatically bound to amino groups while at least another one is distributed within the chitosan structure without clear localization. This obviously decreases the resolution in the NMR spectrum. It is noteworthy that even if water is only present in lower quantity, the structure is not so well resolved.

In CSF7 (Fig. 3), two peaks are present for both carbonyl and methyl groups (as previously observed in Fig. 1). They are attributed to acetate ions (181 and 24.8) and remaining N-acetyl groups (174 and 23.3 ppm). Carbonyl of N-acetyl groups (174 ppm) is correlated with proton atoms in the range of those of the glucosamine unit. It matches in particular the H2 proton (H directly bonded to C2) at 3.4 ppm, in agreement with the structure. This carbonyl group does not show any cross-peak with protons of its bonded methyl certainly because of the fast rotation of the methyl. The carbonyl of the acetate ions only shows a weak correlation with protons of its methyl group (24.8 ppm) at 2.5 ppm. This observation suggests a slower rotation of the methyl in the acetate ion than in the N-acetyl group. It is probable that acetate ions, trapped between chitosan chains form an electrostatic bonding $CH_3COO^-/^+H_3N$-R which hinders the dynamic. This film, in a more hydrated state compared to the previous one, seems to be more uniformly structured as regards to interactions with acetate ions.

In addition, the analysis of the spectra of the glucosamine unit in CSF7 (Fig. 3) allows to identifying four cross peaks associated with four distinct carbon sites for the C1 carbon. The same C1 signal in CSF3 also gives several correlations and three carbon sites are visible. Fig. 1 previously showed that a +3 ppm shift is observed for C1 from CSF3 to CSF7. But, considering the multiplicity of the peak, it seems that it is rather a modification of the relative population of the sites, than a displacement of the line which produces the observed effect of an apparent shift of +3 ppm. In CSF3 the maximum of the signal is centered at 101.1 and 98.6 ppm and the

observed peak at 103.4 ppm presents less intensity. On the contrary in CSF7 the maximum of the signal is observed for site above 103 ppm (104.0 and 105.3 ppm) and less signal is observed below this chemical shift. In CSF7 the two more intense peaks could be associated with the two different sites of C1, as proposed by Ogawa et al. (2004) in proximity with H_2O and the two lower frequency signal are associated with comparable sites but in proximity of acetate ions. In CSF3, since the acetate ions/H_2O ratio is significantly higher, the lower frequency signals are more intense. The same consideration applies to the other carbon of the glycosidic bond (C4).

Carbon atoms in C3 and C6 position also present several overlapping signals because their hydroxyl groups are directly involved in H-bonding and are likely to be exposed to various environments, depending in particular on the included molecules nearby. Carbon atoms in C2 and C5 positions do not exhibit such kind of multiplicity, but the C2 peak seems to be broader than the C5 peak and in Fig. 3, where the C2 signal is more resolved, with an observed shoulder at 55.2 ppm. These two signals for C2 are attributed to the two possible coordinations of bonded nitrogen atoms: primary amine or N-acetylamine. In both films, water or acetate ions do not affect carbons in C5 and C2 position and observed cross-peaks for C5 and C2 are simply associated to direct correlations with their primary hydrogen atoms.

It is worth noting that, albeit very weak, ^{1}H frequency (5–6 ppm) correlations are observed. These chemical shifts, in the range of OH and NH functionalities, have also been noticed by Domján et al. (2009) for C3, C5 and C6. In CSF3, these correlations are obtained at 4.7 for C3 and C5 and at 5.3 for C2, while such correlations are seen at 6.4 ppm for the C3–C5 signal in CSF7. As proposed by Kameda et al. (2005), in chitin, intermolecular hydrogen bonding (between amide protons and carbonyl) as well as a combination of intermolecular (between amide protons and carbonyl) and intramolecular (between carbonyl and hydroxyl on C6) hydrogen bonding take part in stabilizing the structure. Thus, in accordance with this suggested structure, and upon their chemical shifts, we may attribute these 5–6 ppm correlations to the proximity of amide protons to the C5 and C3 located on the same chain or on the closest hydrogen-bonded chain.

4. Conclusions

Chitosan films produced from a 10% acetylated polymer by solvent casting with acetic acid and stored in two different relative humidity environments (32 or 75%) at 20 °C for 1 month, displays significant changes in their ^{1}H–^{13}C CPMAS NMR spectra. In particular, increasing moisture content leads to a decrease in the acetate ions trapped in the interchain structure, which participate in the molecular architecture of polymer by electrostatic interactions. Such changes imply a reorganization of chains as clearly evidenced, not only by the modifications in the populations of acetate ions, but also by the modifications in the local environment of C1 and C4 carbon atoms implied in the glycosidic linkage. This is related to variations in the two torsion angles of this glycosidic bond. FSLG ^{1}H–^{13}C HETCOR brings further information to probe weak interactions over small distances. It also shows a real multiplicity of peaks, especially for carbons involved in the glycosidic linkage, which reveals multiple conformational states.

This work highlights the cruciality of the acetic acid used as acidic medium for chitosan film production and its role as counter ion to stabilize the structure. The relative humidity environment also plays a major role through acetate ions removal from the film. Different structures can therefore be directed by changing the water/acetate ratio taking part in hydrogen bonding network between chitosan chains. Changing the water content in such a system offers thus the possibility to modulate the polymer structure and therefore the controlled release of active compounds from the coating according to the humidity level, such as for medicated dressing or active packaging.

Acknowledgment

This work was supported by the Regional Council of Burgundy through the project number 2012-9201AAO049S780.

References

Brugnerotto, J., Lizardi, J., Goycoolea, F. M., Argüelles-Monal, W., Desbrières, J., & Rinaudo, M. (2001). An infrared investigation in relation with chitin and chitosan characterization. *Polymer*, *42*(8), 3569–3580.

Cárdenas, G., Cabrera, G., Taboada, E., & Miranda, S. P. (2004). Chitin characterization by SEM, FTIR, XRD, and ^{13}C cross polarization/mass angle spinning NMR. *Journal of Applied Polymer Science*, *93*(4), 1876–1885.

Clark, G. L., & Smith, A. F. (1937). X-ray diffraction studies of chitin, chitosan, and derivatives. *The Journal of Physical Chemistry*, *40*, 863–879.

Cunha, R. A., Franca, E. F., Soares, T. A., Rusu, V. H., Pontes, F. J. S., & Lins, R. D. (2012). The molecular structure and conformational dynamics of chitosan polymers: An integrated perspective from experiments and computational simulations. In D. N. Karunaratne (Ed.), *The complex world of polysaccharides* (pp. 229–256). InTech.

Demarger-Andre, S., & Domard, A. (1994). Chitosan carboxylic acid salts in solution and in the solid state. *Carbohydrate Polymers*, *23*(3), 211–219.

Di Martino, A., Sittinger, M., & Risbud, M. V. (2005). Chitosan: A versatile biopolymer for orthopaedic tissue-engineering. *Biomaterials*, *26*(30), 5983–5990.

Domján, A., Bajdik, J., & Pintye-Hodi, K. (2009). Understanding of the plasticizing effects of glycerol and PEG 400 on chitosan films using solid-state NMR spectroscopy. *Macromolecules*, *42*(13), 4667–4673.

Dutta, P. K., Tripathi, S., Mehrotra, G. K., & Dutta, J. (2009). Perspectives for chitosan based antimicrobial films in food applications. *Food Chemistry*, *114*(4), 1173–1182.

Epure, V., Griffon, M., Pollet, E., & Avérous, L. (2011). Structure and properties of glycerol-plasticized chitosan obtained by mechanical kneading. *Carbohydrate Polymers*, *83*(2), 947–952.

Ferreira, M. L., Pedroni, V. I., Alimenti, G. A., Gschaider, M. E., & Schulz, P. C. (2008). The interaction between water vapor and chitosan: II. Computational study. *Colloids and Surfaces A: Physicochemical and Engineering Aspects*, *315*(1–3), 241–249.

Franca, E. F., Lins, R. D., Freitas, L. C. G., & Straatsma, T. P. (2008). Characterization of chitin and chitosan molecular structure in aqueous solution. *Journal of Chemical Theory and Computation*, *4*(12), 2141–2149.

Franca, E. F., Freitas, L. C. G., & Lins, R. D. (2011). Chitosan molecular structure as a function of N-acetylation. *Biopolymers*, *95*(7), 448–460.

Harish Prashanth, K. V., Kittur, F. S., & Tharanathan, R. N. (2002). Solid state structure of chitosan prepared under different N-deacetylating conditions. *Carbohydrate Polymers*, *50*(1), 27–33.

Haxaire, K., Maréchal, Y., Milas, M., & Rinaudo, M. (2003). Hydration of polysaccharide hyaluronan observed by IR spectrometry: I. Preliminary experiments and band assignments. *Biopolymers*, *72*(1), 10–20.

Heux, L., Brugnerotto, J., Desbrieres, J., Versali, M. F., & Rinaudo, M. (2000). Solid state NMR for determination of degree of acetylation of chitin and chitosan. *Biomacromolecules*, *1*(4), 746–751.

Kameda, T., & Ando, I. (1997). The relationship between the helical conformation and ^{13}C NMR chemical shift of amino acid residue carbonyl carbons of polypeptides in the solid state. *Journal of Molecular Structure*, *412*(3), 197–203.

Kameda, T., Takeda, N., Kuroki, S., Kurosu, H., Ando, S., Ando, I., et al. (1996). Hydrogen-bonded structure and ^{13}C NMR chemical shift tensor of amino acid residue carbonyl carbons of peptides and polypeptides in the crystalline state. Part I. *Journal of Molecular Structure*, *384*(1), 17–23.

Kameda, T., McGeorge, G., Orendt, A. M., & Grant, D. M. (2004). C-13 NMR chemical shifts of the triclinic and monoclinic crystal forms of valinomycin. *Journal of Biomolecular NMR*, *29*(3), 281–288.

Kameda, T., Miyazawa, M., Ono, H., & Yoshida, M. (2005). Hydrogen bonding structure and stability of α-chitin studied by ^{13}C solid-state NMR. *Macromolecular Bioscience*, *5*(2), 103–106.

Kono, H. (2004). Two-dimensional magic angle spinning NMR investigation of naturally occurring chitins: Precise ^{1}H and ^{13}C resonance assignment of α- and β-chitin. *Biopolymers*, *75*(3), 255–263.

Kumar, M. (2000). A review of chitin and chitosan applications. *Reactive and Functional Polymers*, *46*(1), 1–27.

Kumirska, J., Czerwicka, M., Kaczyński, Z., Bychowska, A., Brzozowski, K., Thöming, J., et al. (2010). Application of spectroscopic methods for structural analysis of chitin and chitosan. *Marine Drugs*, *8*(5), 1567–1636.

Lertworasirikul, A., Tsue, S.-I., Noguchi, K., Okuyama, K., & Ogawa, K. (2003). Two different molecular conformations found in chitosan type II salts. *Carbohydrate Research*, *338*(11), 1229–1233.

Murata, K., Kono, H., Katoh, E., Kuroki, S., & Ando, I. (2003). A study of conformational stability of polypeptide blends by solid state two-dimensional ^{13}C–^{1}H heteronuclear correlation NMR spectroscopy. *Polymer*, *44*(14), 4021–4027.

Ogawa, K., Yui, T., & Okuyama, K. (2004). Three D structures of chitosan. *International Journal of Biological Macromolecules*, *34*(1/2), 1–8.
Okuyama, K., Noguchi, K., Miyazawa, T., Yui, T., & Ogawa, K. (1997). Molecular and crystal structure of hydrated chitosan. *Macromolecules*, *30*(19), 5849–5855.
Okuyama, K., Noguchi, K., Kanenari, M., Egawa, T., Osawa, K., & Ogawa, K. (2000). Structural diversity of chitosan and its complexes. *Carbohydrate Polymers*, *41*(3), 237–247.
Peter, M. G. (1995). Applications and environmental aspects of chitin and chitosan. *Journal of Macromolecular Science, Part A*, *32*(4), 629–640.
Prathab, B., & Aminabhavi, T. M. (2007). Molecular modeling study on surface, thermal, mechanical and gas diffusion properties of chitosan. *Journal of Polymer Science, Part B: Polymer Physics*, *45*(11), 1260–1270.
Rinaudo, M. (2006). Chitin and chitosan: Properties and applications. *Progress in Polymer Science*, *31*(7), 603–632.
Saito, H., Tabeta, R., & Ogawa, K. (1987). High-resolution solid-state carbon-13 NMR study of chitosan and its salts with acids: Conformational characterization of polymorphs and helical structures as viewed from the conformation-dependent carbon-13 chemical shifts. *Macromolecules*, *20*(10), 2424–2430.
Shahidi, F., Arachchi, J. K. V., & Jeon, Y. J. (1999). Food applications of chitin and chitosans. *Trends in Food Science and Technology*, *10*(2), 37–51.
Sikorski, P., Hori, R., & Wada, M. (2009). Revisit of α-chitin crystal structure using high resolution X-ray diffraction data. *Biomacromolecules*, *10*(5), 1100–1105.
Tanner, S. F., Chanzy, H., Vincendon, M., Roux, J. C., & Gaill, F. (1990). High-resolution solid-state carbon-13 nuclear magnetic resonance study of chitin. *Macromolecules*, *23*(15), 3576–3583.
Van Rossum, B. J., Förster, H., & De Groot, H. J. M. (1997). High-field and high-speed CP-MAS ^{13}C NMR heteronuclear dipolar-correlation spectroscopy of solids with frequency-switched Lee–Goldburg homonuclear decoupling. *Journal of Magnetic Resonance*, *124*, 516–519.
Webster, A., Osifo, P. O., Neomagus, H. W. J. P., & Grant, D. M. (2006). A comparison of glycans and polyglycans using solid-state NMR and X-ray powder diffraction. *Solid State Nuclear Magnetic Resonance*, *30*(3/4), 150–161.
Yui, T., Imada, K., Okuyama, K., Obata, Y., Suzuki, K., & Ogawa, K. (1994). Molecular and crystal structure of the anhydrous form of chitosan. *Macromolecules*, *27*(26), 7601–7605.
Zhang, M., Haga, A., Sekiguchi, H., & Hirano, S. (2000). Structure of insect chitin isolated from beetle larva cuticle and silkworm (Bombyx mori) pupa exuvia. *International Journal of Biological Macromolecules*, *27*(1), 99–105.